AIP Journal of Applied Physics

Epitaxial growth of Pb(Zr0.53Ti0.47)O3 films on Pt coated magnetostrictive amorphous metallic substrates toward next generation multiferroic heterostructures

B. Hu, Y. Chen, A. Yang, S. Gillette, T. Fitchorov, A. Geiler, A. Daigle, X. D. Su, Z. Wang, D. Viehland, and V. G Harris

Citation: Journal of Applied Physics **111**, 064104 (2012); doi: 10.1063/1.3697605
View online: http://dx.doi.org/10.1063/1.3697605
View Table of Contents: http://scitation.aip.org/content/aip/journal/jap/111/6?ver=pdfcov
Published by the AIP Publishing

Epitaxial growth of $Pb(Zr_{0.53}Ti_{0.47})O_3$ films on Pt coated magnetostrictive amorphous metallic substrates toward next generation multiferroic heterostructures

B. Hu,[1,a)] Y. Chen,[1] A. Yang,[1,b)] S. Gillette,[1] T. Fitchorov,[1] A. Geiler,[1] A. Daigle,[1] X. D. Su,[2] Z. Wang,[3] D. Viehland,[3] and V. G Harris[1]

[1]*Center for Microwave Magnetic Materials and Integrated Circuits, and Department of Electrical and Computer Engineering, Northeastern University, Boston, Massachusetts 02115, USA*

[2]*Jiangsu Key Laboratory of Thin Films, Department of Physics, Soochow University, Suzhou 215006, People's Republic of China*

[3]*Department of Materials Science and Engineering, Virginia Tech, 306 Holden Hall, Blacksburg, Virginia 24061, USA*

(Received 9 November 2011; accepted 22 February 2012; published online 22 March 2012)

Piezoelectric films of $Pb(Zr_{0.53}Ti_{0.47})O_3$ (PZT) were deposited by pulsed laser deposition onto metallic magnetostrictive substrates. In order to optimize the growth of PZT films, a buffer layer of Pt was employed, as well as variation of deposition temperature, pressure, and laser energy. Room temperature θ-2θ x-ray diffraction measurements indicate all diffraction features correspond to reflections indexed to a single PZT phase of space group *P4mm*. Scanning electron microscopy images reveal pinhole-free dense films of pyramidal shaped crystal arrangements whose orientation and size were controlled by variation of oxygen pressures during deposition. The resulting PZT films had a value of $d_{33} \sim 46$ pm/V representing a 53% increase over previous efforts to realize a piezoelectric/Metglas^{TM} film heterostructure. © *2012 American Institute of Physics*. [http://dx.doi.org/10.1063/1.3697605]

I. INTRODUCTION

Multiferroic (MF) composites or heterostructures have been used for conversion of magnetic energy to electric energy through strain transfer from magnetostrictive (ferromagnetic) to piezoelectric (ferroelectric) components, and vice versa.[1,2] Because of this unique interplay between magnetic and electric polarization fields, much attention has been paid to understanding the underlying physical and materials science aspect of such systems as well as understanding their engineering potential and utility, such as in transformers, transducers, gyrators, surface acoustic wave devices, filters, sensors, and energy harvesters (among other applications).[3] In nature, single-phase MF materials are rare and include Cr_2O_3, $BiFeO_3$, $Sr_3Co_2Fe_{24}O_{41}$,[4,5] $Ba_{0.5}Sr_{1.5}Zn_2(Fe_{1-x}Al_x)_{12}O_{22}$,[6] and $Ba_2Mg_2Fe_{12}O_{22}$ (Ref. 7) systems among others, and typically demonstrate magnetoelectric (ME) coupling below room temperature. Because of this the applications that employ single phase MF materials have been limited. In contrast, bulk composites of piezoelectric and magnetostrictive materials have shown giant ME (GME) coupling at room temperature. The most common and useful manifestation of such structures have been the piezoelectric/magnetostrictive laminate heterostructure.[8–11] The principle figures of merit (FOMs) include the coupling efficiency, which is measured as the induced field per applied electric field arising from the converse magnetoelectric effect (CME), or the electric field strength induced by magnetic field arising from the ME effect. These FOMs can be further distilled for the specific applications such as $T/\sqrt{Hz}$ for sensors. Much interest has concentrated on magnetic sensors due to low noise floors and high sensitivity.[12] To date, the most refined heterostructures that have been studied for both fundamental physical phenomena as well as for engineering potential include bulk magnetostrictive and piezoelectric elements affixed by epoxy. All components of these designs intrinsically possess degrees of microscopic relaxation — be it magnetic, piezoelectric, or mechanical. The chief limitations of the current FOMs have been mechanical and ferroelectric relaxations.[13,14]

An unique approach to addressing these shortcomings is the idea that ferroelectric materials, such as $BaTiO_3$, $Pb(Zr_{0.53}Ti_{0.47})O_3$, $PbTiO_3$, can be deposited directly on magnetostrictive substrates to form multiferroic heterostructures. The compact size and near ideal interlayer bonding is anticipated to largely eliminate mechanical relaxation and provide significant enhancement in ME coupling. Lead zirconium titanate (PZT) has been a popular choice as a MF component due to its excellent piezoelectric, ferroelectric and dielectric properties.[15–17] Correspondingly, Metglas^{TM} (Refs. 18 and 19) has found popularity as the magnetostrictive component in bulk laminated heterostructures.[20] Among the Metglas^{TM} compositions having relatively high magnetostriction are those that possess permeabilities in the range of 40 000, flexibility, ductility, and importantly, a maximum value of dc-biased effective linear peizomagnetic coefficient.[21] As our selected substrate, due to its amorphous structure, the deposition of PZT must be performed at relatively low temperatures ($<700\,^{\circ}C$) to prevent the crystallization and excessive surface oxidation of Metglas^{TM}.

Here, we demonstrate the epitaxial growth of $Pb(Zr_{0.53}Ti_{0.47})O_3$ (PZT) films on Pt-coated Metglas^{TM} by

[a)]Author to whom correspondence should be addressed. Electronic mail: hu.b@neu.edu.

[b)]Present address: Media Business Unit, Hitachi GST, 5601 Great Oaks Parkway, San Jose, CA 95123, USA

pulsed laser deposition (PLD). The PZT films appear as pinhole-free, dense collections of pyramidal shaped crystals whose orientation and size were controlled by applying different oxygen pressures during deposition. A maximum value of $d_{33} \sim 46$ pm/V was measured from the PZT films which represents a 53% enhancement over previous attempts to realize piezoelectric/magnetostrictive film heterostructures.[22] We propose that, based upon these results, this approach represents a viable pathway toward realizing quasi-two dimensional MF heterostructures allowing for low dielectric loss noise and DC leakage resistance leading to the development of MF-based magnetic field sensors with high sensitivity and low $1/f$ noise floor.

II. EXPERIMENT

A $Pb_{1.15}Zr_{0.525}Ti_{0.475}O_3$ target was made by conventional ceramic techniques. The starting materials, PbO, ZrO, and TiO_2 were mixed, shaped and sintered at 800 °C in air for 3 h. Amorphous Metglas™ foil was buffered with Pt as a diffusion barrier and seed layer having thickness of 75 nm by dc magnetron sputter deposition. PZT films were deposited on Metglas™ substrates by pulsed laser deposition (PLD). The laser was excited by KrF gas with $\lambda = 248$ nm and had an average laser density, 400 mJ/cm^2. The base pressure in the deposition chamber was controlled at 5×10^{-5} Torr. The substrate temperature and oxygen pressure were adjusted from 300 to 750 °C and from 10 to 300 mTorr, respectively. Crystal structure and texture of the resulting films were examined by room temperature x-ray diffraction (XRD) using Cu Kα radiation in a θ-2θ geometry and the surface and cross section morphology were observed by scanning electron microscopy (SEM). The chemical compositions of target and films were determined using energy-dispersive x-ray spectroscopy (EDXS) within the SEM instrument. The magnetostrictive properties for the original Metglas™ and thermally cycled PZT/Metglas™ were measured by a microstrain gauge technique.[23] The ferroelectric properties were measured by polarization hysteresis measurements that employed a triangular signal of frequency 10 kHz. The piezoelectric coefficient d_{33} was measured using a Veeco SPI 3100 piezoelectric force microscope (PFM).

III. RESULTS AND DISCUSSIONS

X-ray diffraction (XRD) spectra for the PZT films deposited on Metglas™ substrates were collected at room temperature using Cu Kα radiation in θ-2θ geometry. The XRD patterns of the PZT films grown on Metglas™ substrates at 650 °C and under different working gas pressures are illustrated in Fig. 1. It is noticed that the PZT films remain as a pure phase structure as oxygen pressure changes from 100 to 300 mTorr.[24] Additionally, the thickness of the films was determined to range from 1−2 μm by surface profilometry. The peak near 39.5 deg (in 2θ) corresponds to the Pt buffer layer. The peaks at 31.2°and 38.3° correspond to (110) and (111) planes of the PZT film, respectively. At an oxygen pressure of 100 to 300 mTorr, the PZT crystal film experiences a strongly crystallographic texture along the ⟨111⟩

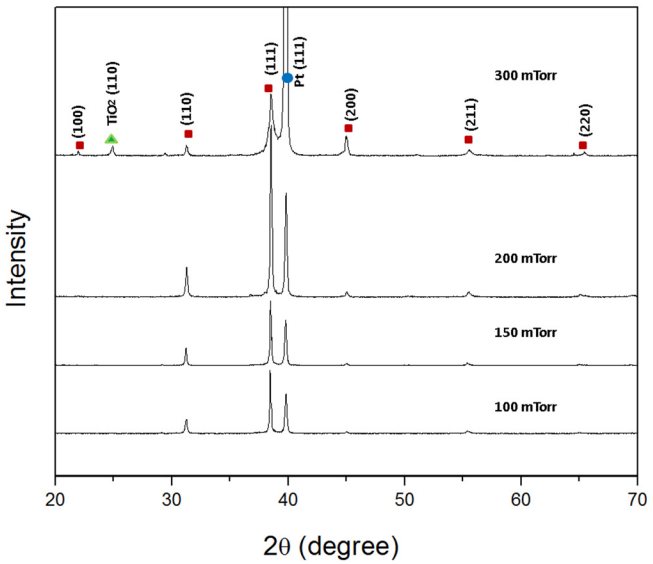

FIG. 1. XRD patterns for PZT films deposited at 650 °C under different oxygen pressures. Diffraction peaks have been identified with either the PZT film or the (111) oriented Pt underlayer.

direction resulting from the epitaxial templating of the Pt (111) oriented buffer layer.

The surface morphology for the PZT films on Metglas™ substrates was observed by scanning electron microscopy (SEM), as shown in Figs. 2(a)–2(f). The SEM images represent the PZT films deposited at 650 °C under 100, 150, 200, and 300 mT O_2 pressure, respectively. The SEM images of the PZT films with a Pt buffer layer resulted in uniform grain growth with pyramidal-shaped grains, reflecting strong (111) orientation. The lattice constant of Pt and PZT crystal is 3.920 and 4.040 Å, respectively. The lattice mismatch between (111) Pt and (111) PZT crystallographic planes is ~2.9%, which is a critical factor in achieving epitaxial growth. Note, by gradually reducing the oxygen pressure, the PZT films tend to form larger grains. The side views of a PZT thin film are presented in Figs. 2(e)–2(f). The sample shown in the Fig. 2(e) was deposited at 300 mTorr of O_2 pressure, and an expanded view is shown in Fig. 2(f). The top layer is the PZT thin film, with Pt as the buffer layer lying in the middle whereas the bottom layer is the Metglas™ substrate. The PZT has a thickness of approximately ~1 μm, which is within the measurement uncertainty of the profilometer trace at 1.1 μm. The side views show abrupt interfaces between each layer, and indicate the PZT film was uniformly deposited on the Metglas™ substrate.

The grain sizes of PZT films were determined by SEM images and XRD Scherrer analysis, as depicted in Fig. 3. The grain size from XRD was derived from the Scherrer equation,

$$B(2\theta) = \frac{K\lambda}{L\cos\theta}, \quad (1)$$

where B is the peak width, and K is a constant with value of 0.94. λ refers to the wavelength of the incident x-ray beam, and L is the grain size. Both XRD and SEM analysis show the same trend. That is, when the pressure is raised the grain size decreases. It is understandable that the mean free path of

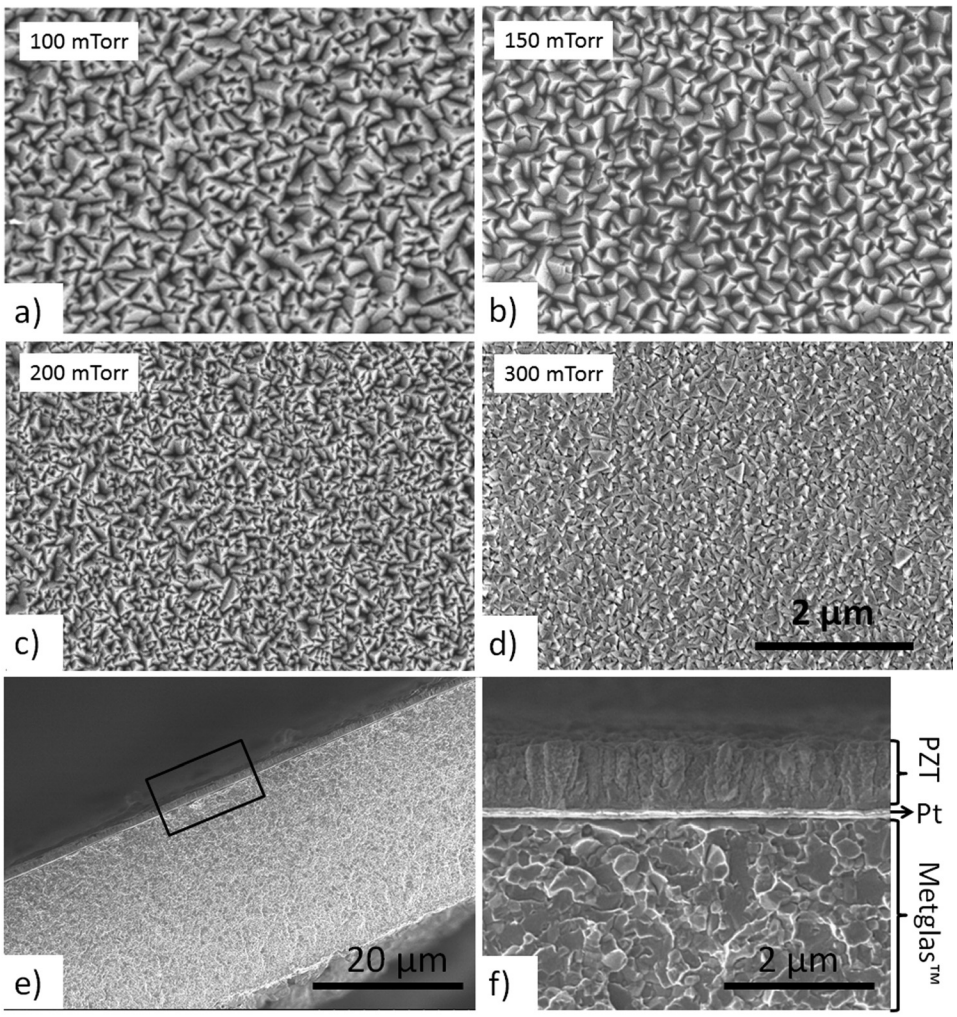

FIG. 2. (a)–(d) SEM surface images of PZT thin films grown at 650 °C under denoted oxygen pressures. (e) SEM cross-section image of film grown at 650 °C and a pressure of 300 mTorr. (f) Expanded view of the selected area of panel (e) denoting the appearance of PZT/Pt/Metglas™ layers.

the ejected particles from the PZT target vary inversely with respect to the working gas pressure P,

$$l = \frac{k_B T}{\sqrt{2}\pi d^2 p}. \quad (2)$$

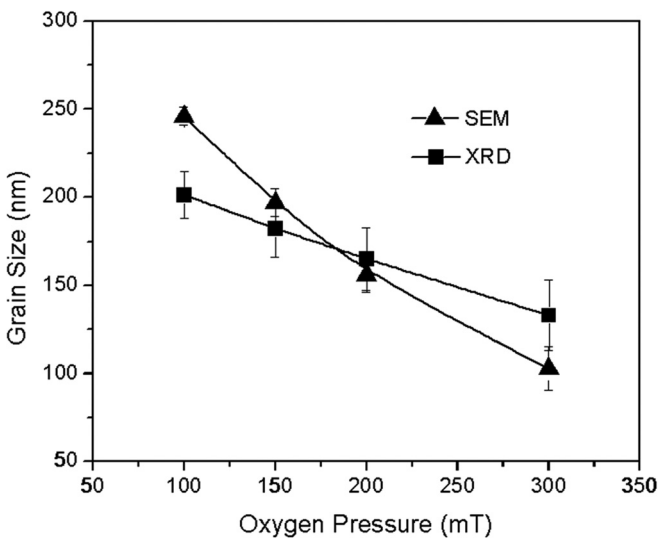

FIG. 3. Average gain size derived from SEM and XRD measurements for PZT films deposited at 650 °C and different oxygen pressures.

Here, l is the free mean path, k_B is the Boltzmann constant, T is temperature, p is pressure, and d is the diameter of the predominant ion in the plasma.[25] In our experiment, the pressure was variable while other parameters were held constant. At lower pressures, the mean free path is larger since the collision between particles during deposition is less than that experienced at higher pressures. With fewer collisions, larger grains form in thicker films. Similar results can be found in the literature.[26]

The chemical composition of the ablated PZT films were determined using energy-dispersive x-ray spectroscopy (EDXS) indicating a stoichiometry of $Pb_{1.0\text{-}1.15}Zr_{0.52}$ $Ti_{0.44\text{-}0.48}O_3$. These values are close to the nominal ratios used in designing the target composition suggesting that preferential ablation and deviation from ideal sticking coefficients did not play a major role.

The magnetostrictive coefficient of the original Metglas™ foil and annealed PZT/Metglas™ heterostructures were measured using a microstrain gauge technique yielding a reduction from $\lambda \sim 27$ to ~ 7 ppm in the Metglas™ as it experienced a thermal cycle during deposition at 650 °C. We attribute this dramatic reduction to the partial crystallization of the amorphous metal substrate. Notwithstanding this result, it is known that the piezomagnetic coefficient ($d\lambda/dH$) has a greater influence upon magnetoelectric coupling than the magnetostriction coefficient. Our previous work has

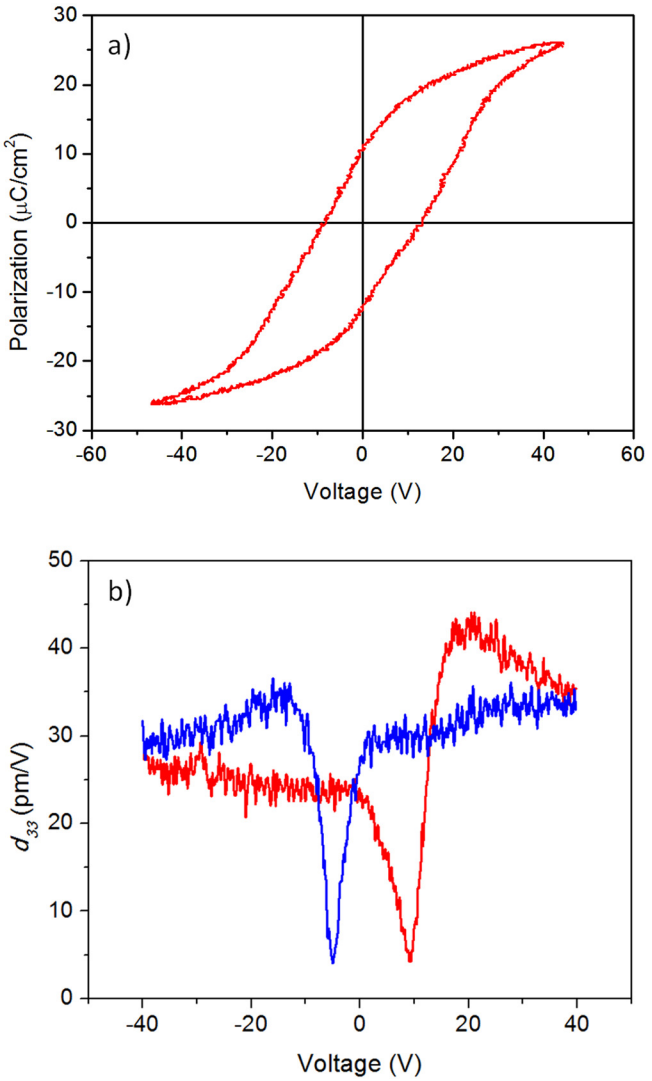

FIG. 4. (a) Polarization hysteresis loop of PZT thin film deposited at 150 mTorr and 650 °C. (b) Piezoelectric measurement of PZT thin film deposited at 150 mTorr O_2 and 650 °C.

demonstrated significant magnetoelectric effects even when the magnetostriction coefficient was about 5 ppm.[2]

Ferroelectric measurements performed on the PLD PZT films yielded the piezoelectric constant d_{33} and polarization hysteresis loop.[27] Fig. 4(a) is a representative ferroelectric hysteresis loop collected under an applied voltage of 50 Vs and with a drive frequency of 10 kHz from the sample grown at 650 °C at a 150 mTorr oxygen pressure. The PZT film was covered by a 400 μm × 400 μm grid and a 150 nm Au electrode was sputter-deposited through the grid. A Au wire having of radius of 25 μm was bonded to the (top) electrode. The PZT film was electrically polarized in the out-of-plane direction. It was found that the saturation polarization and remnant polarization were $P_s \approx 27 \mu C/\text{cm}^2$, and $P_r \approx 10\ \mu C/cm^2$, respectively. These values are in line with those reported for PZT films elsewhere,[28,29] but smaller than that reported for bulk materials.[30] Additionally, PZT crystals have also been shown to display an anisotropic piezoelectric response, showing the lowest saturation polarization along the (111) direction.[31] Nevertheless, the oriented growth of PZT films presents a higher polarization and piezoelectric constant compared to an isotropic polycrystal. In fact, piezoelectric properties not only depend upon crystal orientation but also grain size, film thickness, density, and other physical characteristics.

The pizeoelectric constant d_{33} was measured as a function of applied voltage and is shown in Fig. 4(b). The curve presents a typical butterfly shaped loop, resulting from the nonlinear behavior of the polarization hysteresis curve. As we discussed previously, the ⟨111⟩ orientation of PZT films arises from the epitaxial growth on the (111) Pt buffer layer. It is assumed that the electric domains in the film align under a poling voltage, leading to a substantial increase in polarization[32] and piezoelectric properties. As a result, a piezoelectric coefficient d_{33} ($d_{33} = (\partial S_3/\partial E_3)T$) can be measured due to the induced elongation (strain) under the application of an electric field. Induced charges accumulate on the electrodes and act as a capacitor. With a high dielectric constant, the capacitor tends to gather more charge so as to increase the d_{33}. It was found that at room temperature the extrinsic contribution to the dielectric constant in PZT films was mostly attributed to 180° domain wall motion, which depends upon both film thickness and grain size.[33] The film deposited under 150 mTorr of O_2 pressure gives rise to the maximum value of d_{33} (~46 pm/V) predominantly because of large grain size (average size ~200 nm). Large grain size includes more domain walls, increasing the movement of domain walls exhibited by neighboring grains, so as to contribute a large strain inside the PZT thin film to increase the d_{33} coefficient. A value of $d_{33} \sim 46$ pm/V represents a 53% enhancement compared to previously reported values for BTO film deposited on Metglas™.[15] The high d_{33} in the PZT film benefits from three factors in comparison to the BTO film: (1) the PZT crystal itself has a higher intrinsic d_{33} than that of the BTO crystal, (2) the PZT films described here are of a higher crystallographic quality, and (3) by using smaller top electrodes to reduce the electric leakages through the film.

IV. CONCLUSION

In summary, piezoelectric films of $Pb(Zr_{0.53}Ti_{0.47})O_3$ (PZT) were deposited by pulsed laser deposition onto metallic magnetostrictive substrates. In order to optimize the growth of PZT films, a buffer layer of Pt was employed, as well as variation of deposition temperature, pressure, and laser energy. Room temperature θ-2θ X-ray diffraction measurements indicate all diffraction features correspond to reflections indexed to a single PZT phase of space group *P*4 *mm*. Scanning electron microscopy images reveal pinhole-free dense films of pyramidal shaped crystal arrangements whose orientation and size were controlled by variation of oxygen pressures during deposition. The resulting PZT films had a value of $d_{33} \sim 46$ pm/V representing a 53% increase over previous efforts to realize a piezoelectric/Metglas™ film heterostructure.[15] These results lay the foundation for an alternative pathway to realizing two dimensional multiferroic heterostructures that are low in profile, enhanced ME coupling, and possess the potential to disruptively advance magnetoelectric applications, including transformers, transducers,

gyrators, surface acoustic wave devices, filters, sensors, and energy harvesters.

[1]Y. Chen, A. L. Geiler, T. Fitchorov, C. Vittoria, and V. G. Harris, Appl. Phys. Lett. **95**, 182501 (2009).
[2]Y. Chen, T. Fitchorov, A. L. Geiler, J. Gao, C. Vittoria, and V. G. Harris, Appl. Phys. A **100**, 1149 (2010).
[3]C. Nan, M. Bichurin, S. Dong, and D. Viehland, J. Appl. Phys. **103**, 031101 (2008).
[4]Y. Kitagawa, Y. Hiraoka, T. Honda, T. Ishikura, H. Nakamura, and T. Kimura, Nature Mater. **9**, 797 (2010).
[5]C. Fennie and D. Schlom, Nature Mater. **9**, 787 (2010).
[6]S. Chun, Y. Chai, Y. Oh, D. Jaiswal-Nagar, S. Haam, I. Kim, B. Lee, D. Nam, K. Ko, J. Park, J. Chung, and K. Kim, Phys. Rev. Lett. **104**, 037204 (2010).
[7]N. Kida, S. Kumakura, S. Ishiwata, Y. Taguchi, and Y. Tokura, Phys. Rev. B **83**, 064422 (2011).
[8]A. Mardana, M. Bai, A. Baruth, S. Ducharme, and S. Adenwallab, Appl. Phys. Lett. **97**, 112904 (2010).
[9]W. Eerenstein, N. Mathur, and J. Scott, Nature **442**, 05023 (2006).
[10]C. Chang and G. Carman, J. Appl. Phys. **102**, 124901 (2007).
[11]J. Zhou, W. Zhao, Y. Guo, P. Liu, and H. Zhang, J. Appl. Phys. **105**, 063913 (2009).
[12]Y. Chen, S. Gillette, T. Fitchorov, L. Jiang, H. Hao, J. Li, X. Gao, A. Geiler, C. Vittoria, and V. G. Harris, Appl. Phys. Lett. **99**, 042505 (2011).
[13]Y. Chen, T. Fitchorov, C. Vittoria, and V. G. Harris, Appl. Phys. Lett. **97**, 052502 (2010).
[14]Y. Chen, T. Fitchorov, Z. Cai, K. S. Ziemer, C. Vittoria, and V. G. Harris, J. Phys. D **43**, 155001 (2010).
[15]N. Izyumskaya, Y. I. Alivov, S. Cho, and H. Morkoc, Crit. Rev. Solid State Mater. Sci. **32**, 111 (2007).
[16]X. Wang, Y. Wang, J. Yin, and Z. Liu, Scr. Mater. **46**, 783 (2002).
[17]S. Sriram, M. Bhaskaran, and A. Mitchell, Scr. Mater. **63**, 189 (2010).
[18]J. Ma, J. Hu, Z. Li, and C. Nan, Adv. Mater. **23**, 1062 (2011).
[19]D. Giang, L. Quynh, N. Dung, and N. Hoang Nghi, J. Phys. Conf. Ser. **187**, 012057 (2009).
[20]G. Lawes and G. Srinivasan, J. Phys. D: Appl. Phys. **44**, 243001 (2011).
[21]Y. Yang, J. Gao, Z. Wang, M. Li, J. Li, J. Das, and D. Viehland, Mater. Res. Bull. **46**, 266 (2011).
[22]Z. Wang, L. Yan, Y. Yang, J. Li, J. Das, A. Geiler, A. Yang, Y. Chen, V. G. Harris, and D. Viehland, J. Appl. Phys. **109**, 034102 (2011).
[23]A. Rabinkin, Sci. Technol. Weld. Joining **9**, 181 (2004).
[24]Z. Trajanovic, I. Takeuchi, P. A. Warburton, C. J. Lobb, and T. Venkatesan, Appl. Phys. Lett. **66**, 12 (1995).
[25]S. Chapman and T. G. Cowling, *The Mathematical Theory of Non-uniform Gases*, 3rd. ed. (Cambridge University Press, Cambridge, UK, 1991).
[26]X. D. Zhang, X. J. Meng, J. L. Sun, T. Lin, and J. H. Chu, Appl. Phys. Lett. **86**, 252902 (2005).
[27]R. Lin, T. Wua, and Y. Chu, Scr. Mater. **59**, 897 (2008).
[28]G. Rhun, G. Poullain, R. Bouregba, and G. Leclerc, J. Euro. Ceram. Soc. **25**, 2281 (2005).
[29]M. Dekkers, M. Nguyen, R. Steenwelle, P. te Riele, D. Blank, and G. Rijnders, Appl. Phys. Lett. **95**, 012902 (2009).
[30]Y. Lin, C. Andrews, and H. Sodano, J. Appl. Phys. **108**, 064108 (2010).
[31]Q. Wang, Y. Ding, Q. Chen, and M. Zhao, Appl. Phys. Lett. **86**, 162903 (2005).
[32]J. Yang, S. Mao, K. Yan, and A. Soh, Scr. Mater. **54**, 1281 (2006).
[33]F. Xu, S. Trolier-McKinstry, W. Ren, B. Xu, and Z. Xie, J. Appl. Phys. **89**, 1336 (2001).